Importance of T Cells, Gamma Interferon, and Tumor Necrosis Factor in Immune Control of the Rapid Grower *Mycobacterium abscessus* in C57BL/6 Mice[∇]

Martin Rottman,[1]* Emilie Catherinot,[1] Patrick Hochedez,[1] Jean-François Emile,[2]
Jean-Laurent Casanova,[3] Jean-Louis Gaillard,[1] and Claire Soudais[3]

*Laboratoire de Microbiologie, Hôpital R. Poincaré (AP-HP), and EA 3647, Université de Versailles Saint-Quentin,
Faculté de Médecine Paris-Ile de France-Ouest, 92380 Garches,[1] Laboratoire d'Anatomo-Pathologie,
Hôpital A. Paré (AP-HP), 92100 Boulogne,[2] and Unité d'Immunologie et d'Hématologie,
Hôpital Necker-Enfants Malades (AP-HP), and Laboratory of Human Genetics of
Infectious Diseases, Université René Descartes-INSERM U550, Faculté de
Médecine Necker-Enfants Malades, 75730 Paris cedex 15,[3] France*

Mycobacterium abscessus **is an emerging rapidly growing mycobacterium that causes tuberculous-like lesions in humans. We studied the immune control of this organism in C57BL/6 mice challenged intravenously with 10^7 CFU. Bacteria were eliminated from both the spleen and the liver within 90 days, and liver histology showed organized granulomatous lesions. A T- and B-cell requirement was investigated by challenging $Rag2^{-/-}$, $Cd3\varepsilon^{-/-}$, and $\mu MT^{-/-}$ mice. $Rag2^{-/-}$ and $Cd3\varepsilon^{-/-}$ mice were significantly impaired in the ability to clear *M. abscessus* from the liver and spleen, and $\mu MT^{-/-}$ mice were significantly impaired in the ability to clear *M. abscessus* from the liver, suggesting that infection control was primarily T cell dependent in the spleen and both T and B cell dependent in the liver. The liver granulomatous response was similar to that of wild-type controls in $\mu MT^{-/-}$ mice but completely absent in $Cd3\varepsilon^{-/-}$ and $Rag2^{-/-}$ mice. We studied the involvement of gamma interferon (IFN-γ) and tumor necrosis factor (TNF) by challenging C57BL/6 mice deficient in the IFN-γ receptor ($Ifngr1^{-/-}$) and in TNF ($Tnf^{-/-}$). $Ifngr1^{-/-}$ mice were significantly impaired in *M. abscessus* control both in the spleen and in the liver, and granulomas were profoundly altered. The effect was even more substantial in $Tnf^{-/-}$ mice; they failed to control *M. abscessus* infection in the liver and died within 20 to 25 days after infection with many hepatic inflammatory foci and major lesions of ischemic necrosis in the liver and kidney. These features were not observed with the closely related species *M. chelonae*. T-cell immunity, IFN-γ, and TNF are central factors for the control of *M. abscessus* in C57BL/6 mice, as they are for the control of pathogenic slowly growing mycobacteria.**

Mycobacterium abscessus is a rapidly growing mycobacterium (RGM) that has emerged as a significant pathogen in humans (6, 21) following its recent recognition as a species distinct from *M. chelonae* (36). *M. abscessus* is now recognized as the causative agent of a wide spectrum of human infections, including skin and soft tissue infections (6, 21, 54, 57), lung infections in individuals with or without underlying disorders (e.g., cystic fibrosis) (26, 50), and infections or pseudoinfections related to contaminated medical devices (3, 25, 57). Disseminated infections have also been reported (11) for immunocompromised patients (organ transplantation, autoimmune disorders, malignancies) (6, 28, 48) and for subjects with a genetic defect in the interleukin-12 (IL-12)–gamma interferon (IFN-γ) signaling circuit (9). These life-threatening infections are therapeutically problematic because *M. abscessus* strains are resistant to most antibiotics (6).

In light of clinical data, *M. abscessus* is now considered by many authors to be one of the most pathogenic RGM species (6). However, clear experimental evidence for its pathogenicity is poor; various studies using strains identified as *M. fortuitum* and *M. abscessus* showed that both species were lethal for mice following intravenous injection (35, 47). Little is known about the mechanisms by which *M. abscessus* is controlled in a living host. Byrd and Lyons showed that severe combined immunodeficiency (SCID) mice were more susceptible to *M. abscessus* than wild-type mice in a pulmonary model of infection (7). However, the roles of the B-cell and T-cell responses were not studied. The occurrence of disseminated *M. abscessus* infections in patients with genetic defects in the IL-12–IFN-γ pathway implicates IFN-γ-dependent mechanisms. This is consistent with several histopathological studies in humans showing that *M. abscessus* can cause organized granulomatous lesions with epithelioid giant cells (53). Recent reports of *M. abscessus* infection after use of inhibitors of tumor necrosis factor (TNF) (40, 52) suggested that TNF also contributes to *M. abscessus* control, as demonstrated for other pathogenic mycobacteria (1, 5, 38, 49).

Using the closely related species *M. chelonae* as a control organism, we studied the immune control of *M. abscessus* in C57BL/6 mice. We show here that, in contrast to resistance to *M. chelonae*, resistance to *M. abscessus* absolutely requires adaptive immunity and that T-cell immunity, IFN-γ, and TNF have pivotal roles.

* Corresponding author. Mailing address: Laboratoire de Microbiologie, Hôpital R. Poincaré, 104 Bd Raymond Poincaré, 92380 Garches, France. Phone: 33 1 47 10 46 22. Fax: 33 1 47 10 79 49. E-mail: martin
.rottman@rpc.aphp.fr.

MATERIALS AND METHODS

Mycobacterial strains and growth. *M. abscessus* reference strain CIP 104536[T] (= ATCC 19977[T]) and *M. chelonae* clinical strain A6 (= LRM1262-2000), both provided by the Laboratoire de Référence des Mycobactéries (Institut Pasteur, Paris, France) were used throughout this study. *M. abscessus* CIP 104536[T] is a smooth (S) morphotype strain (10). *M. chelonae* A6 was chosen on the basis of adequate growth at 35°C; type strain CIP 104535 (= ATCC 35752) was unable to grow at temperatures above 32°C. Both strains were passaged twice in mice and cryopreserved at −80°C using cryobeads (Mast Diagnostics, Reinfeld, Germany). Middlebrook 7H9-0.05% Tween medium was first inoculated with a bead and grown aerobically at 35°C with orbital agitation for 72 h. Four vials containing 500 ml of Middlebrook 7H9-0.05% Tween medium were then each inoculated with 2.5 ml of the starter culture and incubated for 18 h. Each culture was harvested by centrifugation, and the pellet washed with phosphate-buffered saline (PBS), resuspended in 50 ml PBS with 10% glycerol, and dissociated by repeated passage through a 29.5-gauge needle. One-milliliter aliquots were frozen at −80°C until they were required and titrated.

Animals. Preliminary experiments comparing the course of *M. abscessus* infection in C57BL/6, DBA/2, and BALB/c mice showed that there was better control of bacteria in C57BL/6 mice than in the other mice in both the liver and the spleen (data not shown). We thus used mice with a C57BL/6 background for our study. Wild-type C57BL/6 mice were purchased from Elevage Janvier (Le Genest Saint-Ile, France). Knockout (KO) mice with a C57BL/6 background (recombinase activating gene 2 [*Rag2*−/−], CD3-epsilon [*Cd3ε*−/−], immunoglobulin μ chain [μ*MT*−/−], IFN-γ receptor chain 1 [*Ifngr1*−/−], and TNF [*Tnf*−/−] mutants) (12, 27, 34, 37, 39, 51) were purchased from Centre de Distribution, Typage et Archivage animal, Orléans, France, and age and gender matched with wild-type C57BL/6 mice. All animals were 8 to 12 weeks old when they were infected, and they were kept in a confinement class II facility under filter covers, placed in single-use cages with irradiated litter, and given irradiated chow and autoclaved water ad libidum. Experiments were conducted in accordance with the guidelines of the animal welfare committee of the Université Versailles Saint-Quentin.

Animal challenge and killing. We prepared the challenge inocula from rapidly thawed frozen aliquots. Bacterial clumps were eliminated by iterative passages through a 29.5-gauge insulin needle (Becton Dickinson), and suspensions were then diluted appropriately in PBS. Mice were inoculated by intravenous injection of 10[7] CFU in 0.2 ml into the lateral tail vein. Groups of five mice were killed at various time points by carbon dioxide narcosis, and the spleen, liver, and left lung were removed aseptically. Experiments were performed two or three times, as specified below.

Enumeration of viable bacteria. For bacterial counting, the organs were placed in 2-ml screw-cap tubes filled with sterile water and homogenized with a mini-8 beadbeater (Biospec, Bartlesville, OK) using a 5-mm stainless steel ball. Fifty-microliter spots of serial fivefold dilutions were plated on Mueller-Hinton agar and incubated at 35°C under a humidified 5% CO_2 atmosphere for 4 days; colonies were then counted using a stereoscopic binocular microscope. The results were expressed as the mean log_{10} CFU per organ. The minimum detection limits were 2 CFU per lung and 170 CFU per spleen or liver.

Histology and immunohistochemistry. Organs were fixed for 24 h by immersion in 3.7% formaldehyde, transferred to 70% ethanol for 24 to 48 h, and then embedded in paraffin. Five-micrometer-thick sections were cut with a rotary microtome, stretched in a water bath, mounted on glass slides, and stained with hematoxylin-eosin-safran (HES) or by the Ziehl-Neelsen method. Slides positive for acid-fast bacilli were included as controls for Ziehl-Neelsen staining. Qualitative analysis of the slides was carried out by an experienced pathologist (J.F.E.) blinded to the nature of the slides examined.

Liver samples to be processed for immunolabeling were embedded in OCT compound (Miles Scientific, Naperville, IL) and frozen in liquid nitrogen. Cryostat sections (thickness, 5 to 7 μm) were cut, fixed in cold acetone for 10 min, and air dried. The sections were blocked with 20% goat serum in PBS for 30 min at room temperature and then incubated with 1:50 dilutions of rat primary antibody (anti-murine CD4, CD8 [eBioscience, San Diego, CA]) for 2 h at room temperature. Labeling was detected with biotinylated rabbit anti-rat immunoglobulin and neutravidin-peroxidase used according to the manufacturer's recommendations (Invitrogen, Cergy Pontoise, France). All incubations were followed by three washes in PBS. Sections were counterstained with Meyer's hematoxylin.

Flow cytometric analysis. Spleen cell suspensions were immunostained, collected on a BD-LSRII instrument (Becton Dickinson), and analyzed with FlowJo software (Tree Star Inc., United States). Anti-TCR-PE-Cy5 and anti-CD8alpha-APC-Cy7 antibodies were obtained from BD-PharMingen (BD Biosciences,

Belgium), and anti-CD4-PE-Texas red was obtained from Caltag (Invitrogen, Cergy-Pontoise, France). 4′,6′-Diamidino-2-phenylindole (DAPI) (Molecular Probes, Invitrogen) was used to exclude dead cells.

Quantitative reverse transcription PCR. Total RNA was isolated from spleens with a QIAGEN RNeasy Protect mini kit with RNase-free DNase set on-column treatment (QIAGEN, Courtaboeuf, France) according to the manufacturer's instructions. An iScript reverse transcription kit (Bio-Rad, Marnes la Coquette, France) was used for reverse transcription. Quantitative PCR was carried out with a Chromo4 instrument (Bio-Rad) using qPCR MasterMix (Eurogentec) and previously described primers and 6-carboxyfluorescein–6-carboxytetramethyl-rhodamine double-dye oligonucleotide probes (Eurogentec, Serain, Belgium) for IFN-γ and TNF (42). An 18S rRNA control kit (Eurogentec) was used to normalize results. Data were quantified with Opticon software according to the manufacturer's recommendations. All signals resulted from amplification of reverse-transcribed RNA, as confirmed by the absence of signals from reactions with RNA extracts before reverse transcription.

Statistical analysis. Fisher's exact test and Student's *t* test were used to analyze the significance of quantitative data; *P* values less than 0.05 were considered significant.

RESULTS

Course of *M. abscessus* and *M. chelonae* infection in C57BL/6 mice. We challenged C56BL/6 mice intravenously with 1×10^6, 1×10^7, and 5×10^7 CFU to determine the dose best suited for analysis of the control of *M. abscessus* infection (Fig. 1A). Challenge with 1×10^7 and 5×10^7 CFU resulted in similar liver burdens, whereas 1×10^6 CFU induced a poorly reproducible histological response. Thus, we used the 1×10^7-CFU dose for comparison of *M. abscessus* and *M. chelonae* growth curves in C57BL/6 mice. We inoculated animals intravenously with each species and then counted the CFU in the lung, spleen, and liver at various times. We report below only the spleen and liver counts as the lung burden of both species remained below the threshold throughout the study. The initial distributions of mycobacteria in the liver and spleen were similar for *M. abscessus* and *M. chelonae*: about 90% of the inoculated CFU were recovered from the liver and about 10% were recovered from the spleen on day 1 (Fig. 1B). The numbers of viable bacteria decreased similarly between days 1 and 15 for the two species, with reductions of 2 log_{10} CFU in the spleen and 3 log_{10} CFU in the liver. However, on day 45 postinfection, *M. abscessus* was still detected, whereas *M. chelonae* was cleared from all animals examined (Fig. 1B), a significant difference as determined by Fisher's exact test ($P < 0.03$).

HES-stained liver sections from animals infected with either *M. abscessus* or *M. chelonae* had granulomas featuring a lymphocytic cuff surrounding a central core rich in macrophages, with rare epithelioid cells from day 15 on (Fig. 2). The largest numbers, sizes, and degrees of differentiation appeared to occur on day 30, and lesions diminished by day 45 in *M. abscessus*- and *M. chelonae*-infected mice. Granulomas tended to be larger with *M. abscessus* than with *M. chelonae* as early as day 15, and this trend was constant throughout the 90 days of the experiment. Examination of lung sections showed no inflammatory reaction following inoculation with either *M. abscessus* or *M. chelonae*, as expected from the absence of bacteria detected by culture. Ziehl-Neelsen-stained slides of spleens and livers did not show evidence of acid-fast bacilli at any time.

T- and B-cell requirement for *M. abscessus* control. The role of functional T and B cells in the control of *M. abscessus* and *M. chelonae* in C57BL/6 mice was studied by challenging *Rag2*−/−, *Cd3ε*−/−, and μ*MT*−/− KO mice with the C57BL/6

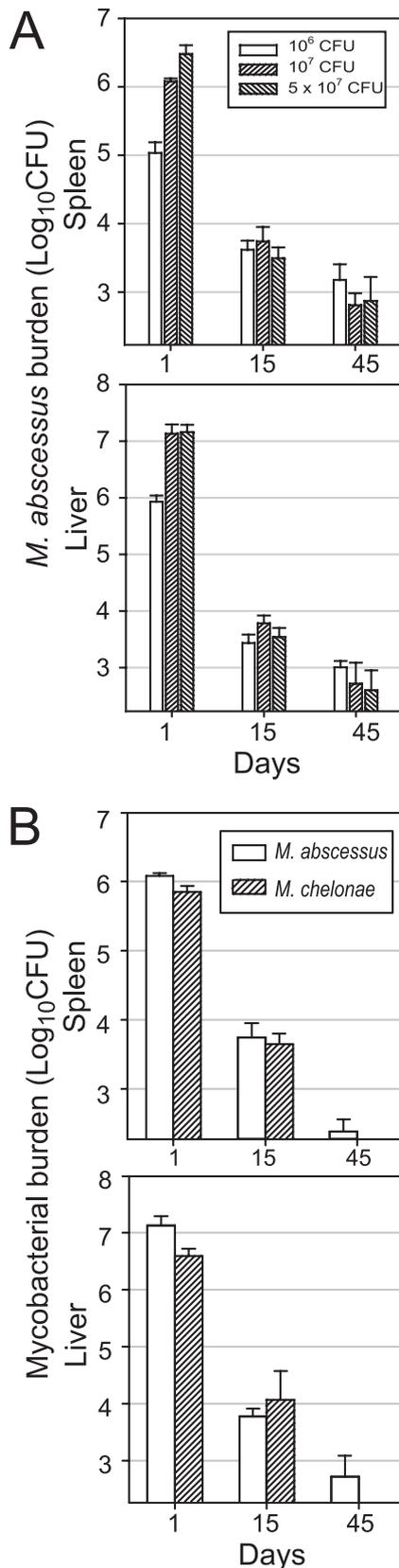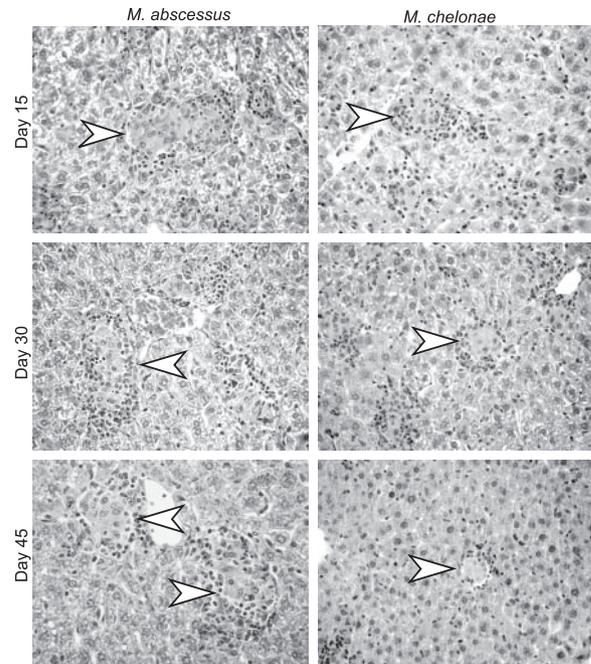A. *M. abscessus* burden (Log₁₀CFU) — Spleen / Liver

FIG. 2. Histopathological analysis of liver sections during infection of wild-type C57BL/6 mice. Animals were inoculated by the intravenous route with 10^7 CFU of *M. abscessus* or *M. chelonae*. HES-stained liver sections (magnification, ×400) obtained on days 15, 30, and 45 after *M. abscessus* or *M. chelonae* challenge are shown. The arrowheads indicate differentiated granulomas featuring an epithelioid core and lymphocytic cuff. Slides were obtained from one of three independent experiments.

background. $Rag2^{-/-}$ and $Cd3\varepsilon^{-/-}$ mice were severely impaired in the ability to control *M. abscessus* infection both in the liver and in the spleen, and the bacterial loads were significantly higher than those of the wild-type controls within 8 days after infection for $Rag2^{-/-}$ mice and within 15 days for $Cd3\varepsilon^{-/-}$ mice (Fig. 3). On day 90, $Cd3\varepsilon^{-/-}$ and $Rag2^{-/-}$ mice still harbored around 10^5 CFU in the spleen and 10^6 CFU in the liver. No death was recorded throughout the study period. The *M. abscessus* counts in the spleens and in the livers of $\mu MT^{-/-}$ mice followed different time courses. The bacterial clearance from $\mu MT^{-/-}$ mouse spleens was similar to the clearance from wild-type mouse spleens throughout the study period. In contrast, the bacterial loads in the liver were as high in $\mu MT^{-/-}$ mice as in $Cd3\varepsilon^{-/-}$ and $Rag2^{-/-}$ mice up to day 30; the load then sharply declined between day 30 and day 45, reaching the same level ($\sim 10^3$ CFU) as the level in wild-type controls on day 45. Surprisingly, the CFU counts on day 90 were extremely diverse, with individual animals having counts from <170 CFU (detection limit) to >10^6 CFU; all animals appeared to be in good health. Unexpectedly, mice that were culture positive for mycobacteria on day 90 yielded colonies of the rough (R) morphotype and colonies of the original S mor-

B. Mycobacterial burden (Log₁₀CFU) — Spleen / Liver

FIG. 1. Infection of wild-type C57BL/6 mice. (A) *M. abscessus* dose response. Mice were injected intravenously with 10^6, 10^7, and 5×10^7 CFU. (B) *M. abscessus* and *M. chelonae* growth curves. Mice were injected intravenously with 10^7 CFU of *M. abscessus* or *M. chelonae*.

The data shown are from one of three independent experiments (means ± standard deviations for log₁₀ CFU per organ; four or five mice per group per time point).
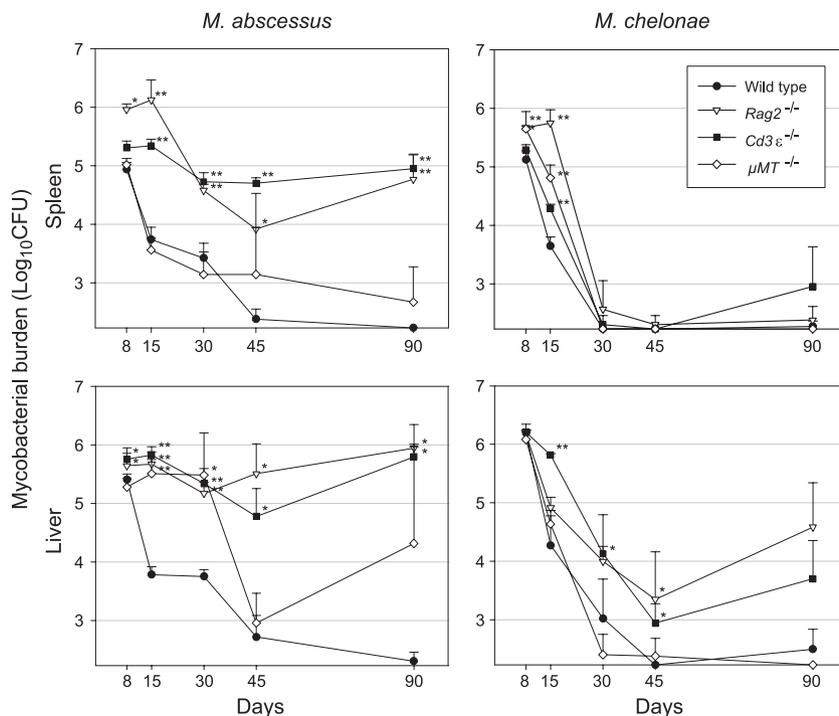
FIG. 3. Infection of mice defective in B- and/or T-cell functions. Wild-type and selectively deficient $Cd3\varepsilon^{-/-}$, $\mu MT^{-/-}$, and $Rag2^{-/-}$ mice with the C57BL/6 background were injected intravenously with 10^7 CFU of *M. abscessus* or *M. chelonae*. The data shown are from one of two independent experiments (means ± standard deviations for $\log_{10}$ CFU per organ; four or five mice per group per time point). The significance of differences between selectively deficient mice and wild-type controls is indicated as follows: one asterisk, $0.001 < P < 0.05$; two asterisks, $P < 0.001$. Note that *M. abscessus* colonies recovered from the liver of $\mu MT^{-/-}$ mice on day 90 exhibited mixed S and R morphotypes at 3/1 to 1/3 ratios.

photype, suggesting that some *M. abscessus* CIP 104536^T cells switched to an R form in the $\mu MT^{-/-}$ mice. To investigate this finding, groups of six $\mu MT^{-/-}$ and wild-type mice were infected and killed 12 months after the challenge. All wild-type controls and four of the six $\mu MT^{-/-}$ mice were negative for *M. abscessus*, but two $\mu MT^{-/-}$ mice had liver counts of 1.3×10^5 and 4.2×10^3 CFU featuring colonies of R and S morphotypes at ratios of 3/1 to 1/3. The regrowth phenomenon observed in the livers of various animals 3 months after infection was thus found to be stable over time and to be associated with the emergence of R forms.

The growth curves for *M. chelonae* were strikingly different. This species was almost entirely cleared from the spleen within 30 days after infection of both KO and wild-type mice, but there were differences during the first few weeks of infection. The bacterial clearance from $Rag2^{-/-}$ mice was significantly worse than that from $\mu MT^{-/-}$ mice, the bacterial clearance from $\mu MT^{-/-}$ mice was significantly worse than that from $Cd3\varepsilon^{-/-}$ mice, and the bacterial clearance from $Cd3\varepsilon^{-/-}$ mice was significantly worse than that from wild-type mice (Fig. 3). Bacterial clearance from the liver was complete in $\mu MT^{-/-}$ mice and wild-type mice on day 90, but the liver counts were 10^4 CFU in both $Cd3\varepsilon^{-/-}$ mice and $Rag2^{-/-}$ mice at this time point and there was no significant difference between these two KO mouse lines.

After challenge with either *M. abscessus* or *M. chelonae*, $\mu MT^{-/-}$, mice produced granulomas undistinguishable from those in wild-type controls as determined by examination of liver sections. In contrast, the histology of infected $Cd3\varepsilon^{-/-}$ or

$Rag2^{-/-}$ mice remained identical to that of uninfected controls throughout the experiment, and there was no detectable recruitment of inflammatory cells at any stage. Thus, the lack of functional T cells was associated with an absence of visible inflammatory foci during *M. abscessus* and *M. chelonae* infection. Ziehl-Neelsen staining of slides did not show mycobacteria in lymphocyte-deficient mice and in wild-type controls.

Overall, these experiments show that functional lymphocytes are absolutely required for the control of *M. abscessus* in C57BL/6 mice and suggest that infection control is primarily T cell dependent in the spleen and both T and B cell dependent in the liver. In contrast, the control of *M. chelonae* infection appears to rely mainly on innate immunity, with possible early involvement of B cells in the spleen. Functional T cells are required for complete *M. chelonae* clearance from the liver.

T-cell, IFN-γ, and TNF responses to *M. abscessus* and *M. chelonae* infection in C57BL/6 mice. Immunohistochemical staining of liver slides from day 30 of *M. abscessus* infection confirmed the presence of CD4$^+$ and CD8$^+$ cells in the periphery of the granulomas (data not shown). We analyzed the T-cell response to infection with *M. abscessus* and *M. chelonae* in the spleen on days 15 and 45. Flow cytometric analysis of the splenic content of TCR$^+$ CD4$^+$ and TCR$^+$ CD8$^+$ cells (Fig. 4A) indicated that there were more CD4$^+$ cells in *M. abscessus*-infected mice than in noninfected controls (16.23% more; $P = 2.06 \times 10^{-5}$) and in *M. chelonae*-infected mice (12.65% more; $P = 9.61 \times 10^{-7}$). In contrast, *M. chelonae*-infected mice had slightly more CD4$^+$ cells (3.58% more; $P = 3.58 \times 10^{-2}$) than noninfected controls. The splenic content of CD4$^+$ cells
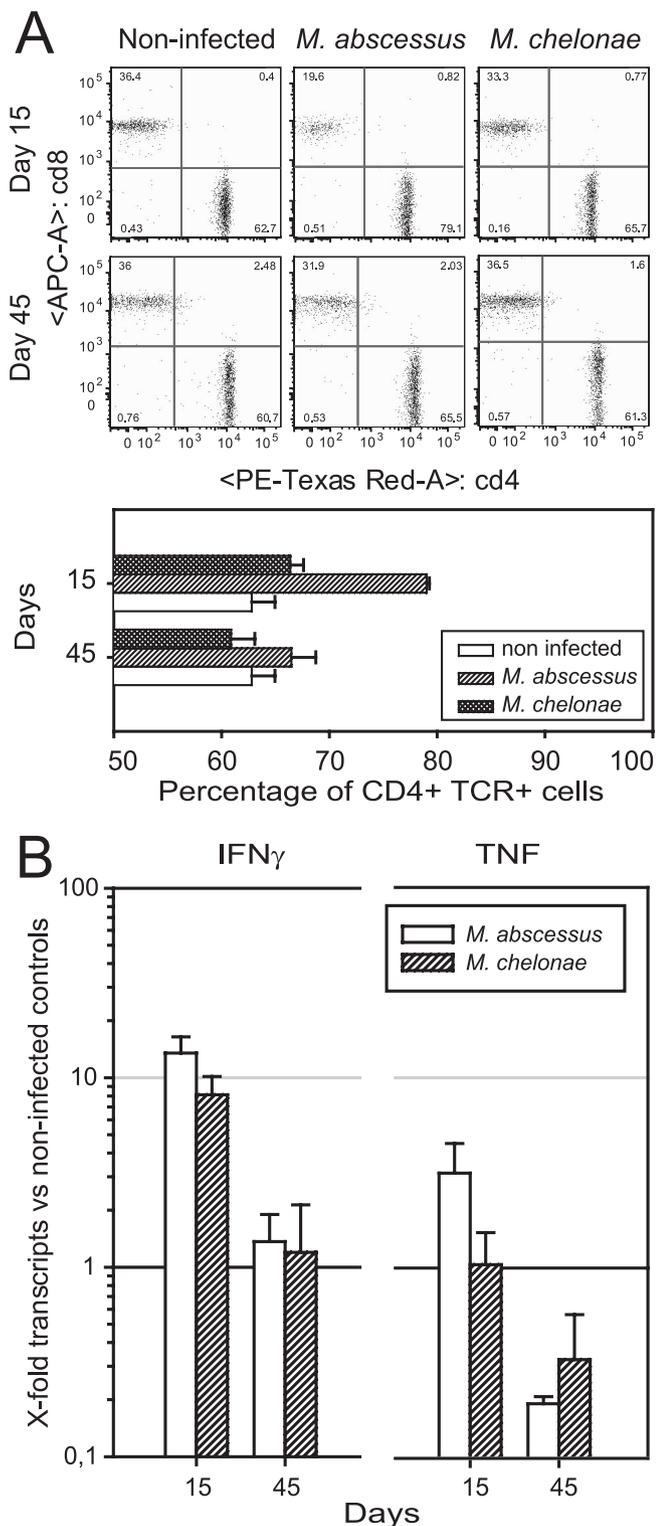
A

returned to the baseline with time in *M. abscessus*-infected mice, and the values were similar to those of noninfected controls by day 45.

Quantification of mRNA transcripts encoding IFN-γ by quantitative reverse transcription PCR (Fig. 4B) showed that *M. abscessus* and *M. chelonae* elicited similar responses; at 15 days after challenge, the transcript levels were 10 times higher than the levels in noninfected controls, and the levels returned to the baseline by day 45. Only *M. abscessus* elicited a significant response in the TNF mRNA level, which was three times higher on day 15 than the level in noninfected controls ($P = 0.012$). Later in the course of the infection, on day 45, *M. abscessus*-infected mice had a significantly lower TNF transcript level than noninfected controls ($P = 0.018$). The levels of TNF transcripts were significantly higher with *M. abscessus* than with *M. chelonae* ($P < 0.04$), and there was a significant decrease between days 15 and 45 ($P < 0.01$).

Roles of IFN-γ and TNF in the control of *M. abscessus*. We used *Ifngr1*$^{-/-}$ and *Tnf*$^{-/-}$ KO mice to investigate the roles of IFN-γ and TNF. Selectively deficient mice and wild-type controls were challenged intravenously with *M. abscessus* or *M. chelonae*, and infection was followed over time by counting CFU and analyzing liver histology.

There was a significant difference between *Ifngr1*$^{-/-}$ mice and *Ifngr1*$^{+/+}$ control mice in both the spleen and the liver 15 days after challenge with *M. abscessus* (Fig. 5); the CFU counts were ~1 $\log_{10}$ higher throughout the course of infection in the spleens and livers of *Ifngr1*$^{-/-}$ animals, and viable bacteria had not been completely cleared from both organs 90 days after the challenge. These findings implicate involvement of IFN-γ in both the early and later stages of infection. However, the *M. abscessus* load decreased steadily despite the absence of IFN-γ signaling, hinting that there are IFN-γ-independent control mechanisms. Consistent with our previous results obtained with selectively lymphocyte-deficient mice, the spleens and livers of *M. chelonae*-infected *Ifngr1*$^{-/-}$ mice responded differently (Fig. 5). The loads in the spleen were not significantly different for the *Ifngr1*$^{-/-}$ and *Ifngr1*$^{+/+}$ mice throughout the observation period, whereas the loads in the liver were significantly higher in *Ifngr1*$^{-/-}$ mice than in *Ifngr1*$^{+/+}$ mice on days 15 and 30. *M. chelonae* was entirely cleared from the spleens of both *Ifngr1*$^{-/-}$ and *Ifngr1*$^{+/+}$ mice on day 90, whereas it was recovered from the livers of all but one *Ifngr1*$^{-/-}$ mouse on day 90.

Liver histology of *Ifngr1*$^{-/-}$ mice (Fig. 6) challenged with *M. abscessus* showed that there were inflammatory cell clumps with no macrophage-rich cores on day 15. A granulomatous architecture appeared on day 30, and there was an irregular lymphocytic cuff surrounding pigmented macrophages. The granulomas in *Ifngr1*$^{-/-}$ mice involuted faster than those in *Ifngr1*$^{+/+}$ mice and had only a few residual pigment-loaded macrophages by day 45 (Fig. 6). *Ifngr1*$^{-/-}$ mice infected with

B

FIG. 4. Host response to infection in wild-type C57BL/6 mice. (A) CD4$^+$ and CD8$^+$ T-cell response. Animals were inoculated by the intravenous route with 10^7 CFU of *M. abscessus* or *M. chelonae*, and the splenic content in TCR$^+$ CD4$^+$ and TCR$^+$ CD8$^+$ cells was analyzed by flow cytometry on days 15 and 45. Experiments were repeated three times. Each dot plot is the plot for one of four mice studied. The lower graph shows the means ± standard deviations of the percentages for cells obtained from four mice in one experiment. (B) Generation of IFN-γ and TNF mRNA transcripts. Transcripts were isolated from infected spleens

on days 15 and 45 and were quantified by quantitative reverse transcription PCR. The results are expressed as the ratio of the expression levels in infected mice to the expression levels in noninfected mice ($n = 4$). The data are from one of two independent experiments.
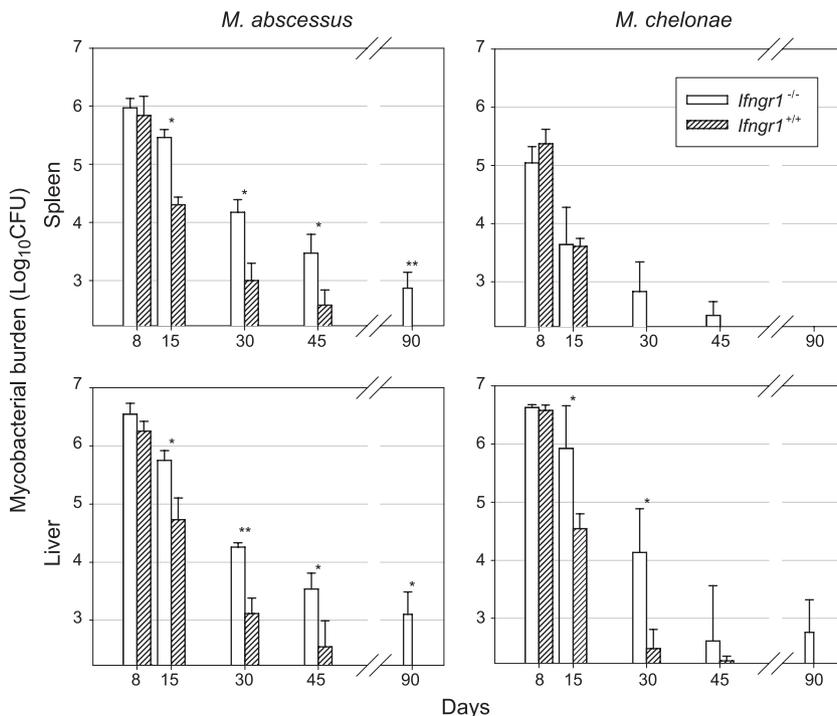
FIG. 5. Infection of *Ifngr1*$^{-/-}$ mice. *Ifngr1*$^{-/-}$ mice and wild-type controls were injected intravenously with 10^7 CFU of *M. abscessus* or *M. chelonae*. The data are from one of three independent experiments (means ± standard deviations of $\log_{10}$ CFU per organ; four or five mice per group per time point). The significance of differences between *Ifngr1*$^{-/-}$ mice and wild-type controls is indicated as follows: one asterisk, $0.001 < P < 0.05$; two asterisks, $P < 0.001$.
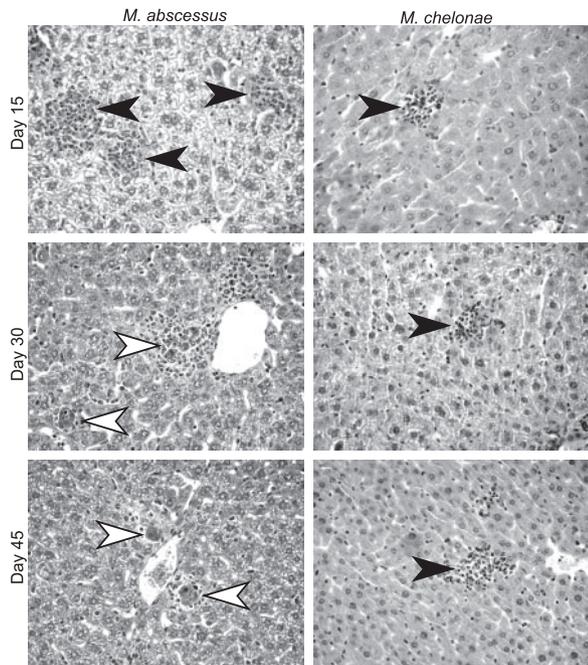

FIG. 6. Histopathological analysis of liver sections of infected *Ifngr1*$^{-/-}$ mice. Animals were inoculated by the intravenous route with 10^7 CFU of *M. abscessus* or *M. chelonae*. HES-stained liver sections (magnification, ×400) obtained on days 15, 30, and 45 after *M. abscessus* or *M. chelonae* challenge are shown. The filled arrowheads indicate undifferentiated inflammatory infiltrates; the open arrowheads indicate differentiated granulomas featuring an epithelioid core and lymphocytic cuff. Slides were obtained from one of three independent experiments.

M. chelonae had inflammatory cell clumps that did not mature into granulomatous architecture (Fig. 6).

Unexpectedly, the control of *M. abscessus* was dramatically altered in mice deficient in TNF. *Tnf*$^{-/-}$ mice infected with *M. abscessus* began to die on day 20 following the intravenous challenge, whereas *Tnf*$^{-/-}$ mice receiving the same challenge of *M. chelonae* were asymptomatic at this time and remained healthy throughout the 90-day observation period (Fig. 7A). The early death of *M. abscessus*-infected *Tnf*$^{-/-}$ mice prompted us to repeat our experiments with CFU determinations after 8, 15, and 21 days (Fig. 7B). Differences in CFU counts between *Tnf*$^{-/-}$ mice and *Tnf*$^{+/+}$ controls were significant by day 8 in the liver and by day 15 in the spleen, and the values were ~2 $\log_{10}$ CFU in the spleen and ~4 $\log_{10}$ CFU in the liver on day 21 (Fig. 7B). Moreover, *M. abscessus* multiplied in the livers of *Tnf*$^{-/-}$ mice between days 15 and 21 (~1-$\log_{10}$ CFU increase). The CFU counts in *Tnf*$^{-/-}$ and *Tnf*$^{+/+}$ mice were similar at all times in both the spleen and the liver (Fig. 7B), indicating that TNF contributes little to the control of *M. chelonae*.

Liver histology analysis of *Tnf*$^{-/-}$ mice infected with *M. abscessus* showed diffuse inflammatory infiltrates evolving into pericentrolobular hepatitis during the infection (Fig. 8A, C, and E). There were apoptotic hepatocytes near the inflammatory foci on day 8 (Fig. 8B). Hepatocyte apoptosis was not observed at later stages, and large areas of ischemic necrosis developed (Fig. 8D). On day 21, shortly before the expected death of the mice, pathological samples showed the presence of large thrombi obtruding major vessels in the liver and kid-
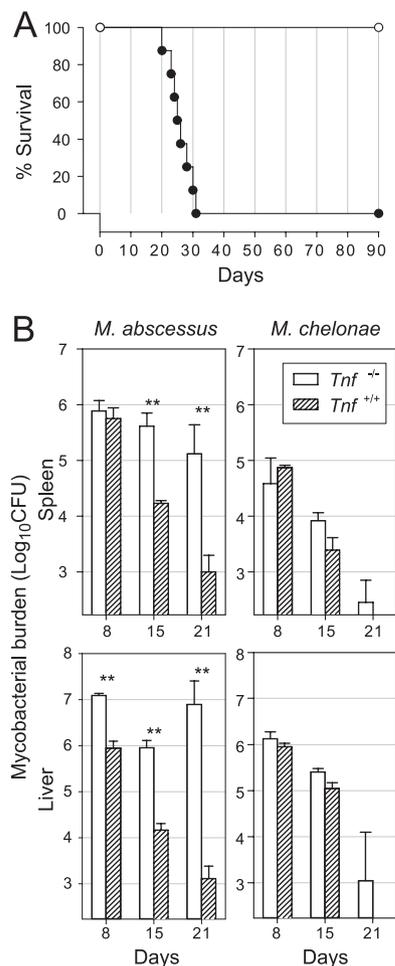
FIG. 7. Infection of $Tnf^{-/-}$ mice. (A) Lethality for animals. Groups of eight $Tnf^{-/-}$ mice were intravenously challenged with 10^7 CFU of *M. abscessus* (●) or *M. chelonae* (○). Infection with *M. abscessus* was lethal within 30 days, whereas infection with *M. chelonae* was asymptomatic up to day 90. The data are from one of three independent experiments. (B) Growth curves. $Tnf^{-/-}$ mice and wild-type controls were injected intravenously with 10^7 CFU of *M. abscessus* or *M. chelonae*. The data are from one of three independent experiments (means ± standard deviations of $\log_{10}$ CFU per organ; four or five mice per group per time point). The significance of differences between $Tnf^{-/-}$ mice and wild-type controls is indicated as follows: one asterisk, $0.001 < P < 0.05$; two asterisks, $P < 0.001$.

ney, arguing that death was at least partially due to massive thromboembolic disease (Fig. 8F).

DISCUSSION

We report here the first detailed study of the immune control of *M. abscessus* in the murine host. We chose to compare *M. abscessus* to *M. chelonae*, a closely related (45) but distinct, species (36) that consistently appears to be much less frequently encountered in human infections than *M. abscessus* (6). We feel that this choice was vindicated by the highly significant differences that we observed between these two species. Our results were fully consistent with a higher pathogenicity of *M. abscessus* (6, 56); in particular, adaptive immunity was essential for the murine host to control *M. abscessus*
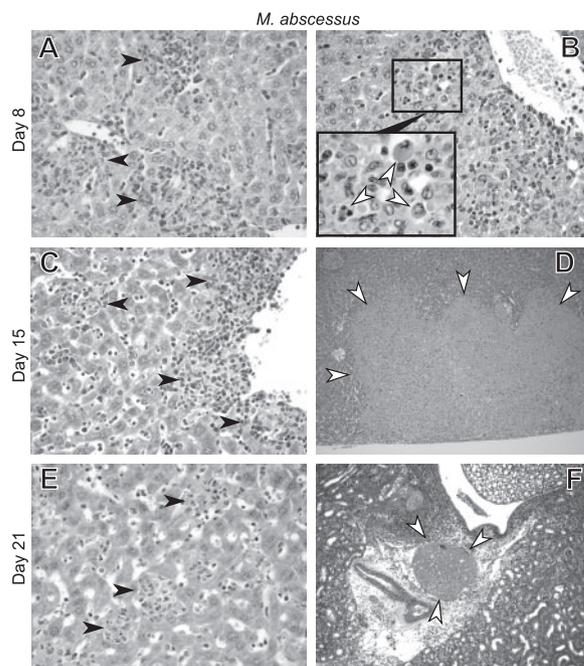

FIG. 8. Histopathological analysis of infected $Tnf^{-/-}$ mice. Animals were inoculated by the intravenous route with 10^7 CFU of *M. abscessus*. HES-stained liver (A to E) and kidney (F) sections obtained on days 8 (A and B), 15 (C and D), and 21 (E and F) are shown. The filled arrowheads indicate undifferentiated inflammatory infiltrates (A, C, and E) (magnification, ×400); the open arrowheads indicate (B) apoptotic hepatocytes on day 8 (magnification, ×200; additional ×4 digital enlargement of the area in the box), (D) ischemic necrosis of the liver on day 15 (magnification, ×100), and (F) thrombosis of the renal vein on day 21 (magnification, ×200). Slides were obtained from one of three independent experiments.

infection, whereas *M. chelonae* control appeared to be much easier and mainly dependent on innate immunity. As observed for intravenous challenge with *M. smegmatis* (46), 90% of the bacteria were localized in the liver and only 10% were localized in the spleen. In contrast to several clinical reports (6, 26, 50), we did not find any particular ability of *M. abscessus* to become established in the lungs. We were unable to recover *M. abscessus* and *M. chelonae* from lung tissue after intravenous challenge, and neither species caused detectable lung tissue lesions. By comparison, intravenous challenge of mice with *M. tuberculosis* or *M. avium* initially leads to bacterial growth in the lungs, spleen, and liver during the first few weeks after challenge, and there is spontaneous resolution in all organs but the lungs (15, 17, 20); such *M. tuberculosis* infections are ultimately lethal (17). Our findings are consistent with a previous report that it is impossible to induce a true *M. abscessus* lung infection by challenging immunocompetent mice by the intratracheal route (7). Our findings are also in line with the occurrence of *M. abscessus* lung disease in patients with preexisting lesions of the respiratory tract (e.g., cystic fibrosis or bronchiectasis). This suggests that more appropriate animal models mimicking clinical situations (e.g., cystic fibrosis) should be used to investigate the mechanisms of *M. abscessus* lung infection.

The role of adaptive immunity in the control of slowly growing mycobacteria (SGM) has been widely studied in intrave-

nous infection models using SCID mice and mice selectively deficient in RAG. The growth of virulent *M. tuberculosis* strains in the spleen, liver, and lungs of SCID mice following intravenous challenge is exponential. The growth of *M. bovis* BCG is slower but still progressive, whereas growth of the attenuated *M. tuberculosis* strain H37Ra is controlled in both SCID and wild-type mice (41). Virulent strains of *M. avium* behave identically in the spleens of SCID and wild-type C57BL/6 mice for the first few weeks of infection. However, the bacterial counts in the spleens of SCID mice continue to increase after 8 weeks of infection, by which time the counts begin to decline in wild-type C57BL/6 mice (15). As observed for *M. tuberculosis* complex (41) and virulent strains of *M. avium* (15), *M. abscessus* is poorly controlled in RAG mice inoculated intravenously; high bacterial counts persist from day 30 on. Similar data have been reported by Bird and Lyons for a respiratory model of *M. abscessus* infection in SCID mice with wild-type BALB/c controls (7). Thus, adaptive immunity is an absolute requirement for the control of *M. abscessus*, a feature shared with pathogenic SGM.

Comparative analysis of bacterial growth curves obtained with $Rag2^{-/-}$, $Cd3\varepsilon^{-/-}$ and $\mu MT^{-/-}$ KO mice clearly showed that control of *M. abscessus* infection relies primarily on T-cell immunity, a finding which has been abundantly documented for SGM (22). Indeed, $Cd3\varepsilon^{-/-}$ and $Rag2^{-/-}$ mice are both severely impaired in the ability to clear *M. abscessus* infection; bacterial loads persist 3 months after challenge ($\sim 10^5$ CFU in the spleen and $\sim 10^6$ CFU in the liver for both types of KO mice), whereas bacteria have been cleared from wild-type mice by that time. The involvement of T-cell immunity was also supported by our analysis of the splenic T-cell response during *M. abscessus* infection, with generation of a TCR^+ $CD4^+$ cellular response on day 15. Although our study is the first study to establish the T-cell dependence of the immune response to an RGM species, it has not been demonstrated that this trait is unique to *M. abscessus*. We showed that an *M. chelonae* control was largely unaffected by the loss of T-cell function, especially in the spleen. This suggests that the behavior of *M. abscessus* differs from that of other RGM species. However, other studies including more RGM species would have to be performed to clarify this issue.

B-cell immunity plays a minor role compared to the role of T-cell immunity, but it is nonetheless involved in the early control of SGM infections in the mouse. It has been shown that $\mu MT^{-/-}$ mice challenged intravenously with 10^6 CFU of *M. tuberculosis* or *M. bovis* BCG had eightfold-higher bacterial counts than wild-type controls up to 6 weeks postinfection, although there were no significant differences between the two mouse lines at later times (55). Studies using respiratory challenge with *M. tuberculosis* have failed to provide evidence of any consistent growth difference, but B cells appear to facilitate dissemination outside the lung and to mitigate the severity of pathological lesions (4, 29). In contrast to observations with SGM, we found that the ability of $\mu MT^{-/-}$ mice to control *M. abscessus* was highly abnormal; the abnormality involved only the liver, where the bacterial loads were 100 times higher than those in wild-type controls on days 15 and 30 postinfection. Bacterial loads in the spleen were similar in $\mu MT^{-/-}$ mice and wild-type controls, arguing against a major role for B cells in this organ. However, the observation that there were signifi-

cantly higher loads in the spleens of $Rag2^{-/-}$ mice than in the spleens of $Cd3\varepsilon^{-/-}$ mice at the early stages indicates that there may be B-cell-mediated control in the spleen. This effect is unmasked in the spleen only in the absence of the much more potent T-cell-mediated immunity, as hinted at by comparative analysis of bacterial growth curves in $\mu MT^{-/-}$ and $Cd3\varepsilon^{-/-}$ mice.

The mechanisms by which B cells may affect the course of mycobacterial infections are believed to involve enhanced antigen presentation, Th1-Th2 bias of the T-cell response, or opsonizing or neutralizing antibodies directed against bacteria or bacterial products (8). Any of these mechanisms may be involved in the case of *M. abscessus*. It is, however, puzzling that R-morphotype variants of *M. abscessus* were found only in $\mu MT^{-/-}$ mice. R variants from *M. abscessus* CIP 104536^T have recently been shown to have lost the ability to produce glycopeptidolipids (GPLs) (10). The emergence of such R variants in $\mu MT^{-/-}$ mice thus suggests that GPLs are major targets of B-cell-mediated immunity to *M. abscessus*. GPLs can make up as much as 70% of the lipids exposed at the mycobacterial surface (2) and have been shown to elicit production of high antibody levels during mycobacterial infections in humans (33). Although our results clearly show the importance of B-cell-mediated immunity for *M. abscessus* control, we must emphasize that they were obtained in an intravenous challenge model with a large bacterial inoculum. Consequently, these findings are in no way predictive of the role of B cells in models with smaller challenge doses or with other routes of administration. It is similarly difficult to extrapolate our results to humans, all the more so because we have no knowledge of any report of *M. abscessus* infection in the context of a humoral deficit.

The role of IFN-γ in antimycobacterial immunity is different in different mycobacterial species, as judged by studies using mice deficient in either IFN-γ or IFN-γ receptor (13, 23). $Ifngr1^{-/-}$ mice are highly susceptible to *M. bovis* BCG and die within 9 weeks of a challenge (30). The course of infection is for the most part similar to that in wild-type controls during the first few weeks, but mycobacteria then grow unrestrictedly in $Ifngr1^{-/-}$ mice, following the same pattern that is observed in SCID mice (41). Data for *M. avium* during the chronic stage of infection also suggest that IFN-γ has a major role, with unrestrained mycobacterial growth but no reported lethality 11 weeks postinfection in IFN-γ-deficient mice (15). Ehlers and Richter classified 13 recently described nontuberculous mycobacteria on the basis of their behavior in IFN-γ-deficient mice and isogenic BALB/c controls as follows: (i) bacteria growing in the spleens of both IFN-γ-deficient and wild-type mice; (ii) bacteria eliminated from wild-type mice but growing in IFN-γ-deficient mice; and (iii) bacteria eliminated even from IFN-γ-deficient mice (20). Only one RGM, *M. confluentis*, was assayed and was shown to be cleared from the spleens of both wild-type and IFN-γ-deficient mice within 4 weeks (20). This study and our experience with *M. abscessus* and *M. chelonae* support the view that *M. abscessus* is likely to be one of the few RGM requiring IFN-γ for adequate control. However, the IFN-γ response is moderate and does not appear to be as crucial for *M. abscessus* as it is for pathogenic SGM (particularly *M. tuberculosis* and *M. avium*) or even for the attenuated pathogen *M. bovis* BCG, because *M. abscessus* is contained in

Ifngr1$^{-/-}$ mice. The increase in IFN-γ transcripts was shown to be transient and moderate following infection with either *M. abscessus* or *M. chelonae*, compared to the long-lasting 100-fold increase observed following infection with *M. tuberculosis* (32). The "intermediate" requirement for IFN-γ for clearance of *M. abscessus* is entirely consistent with clinical data. There have been several reports of disseminated *M. abscessus* infections in patients with defects in the IL-12–IFN-γ circuit, both inherited (16) and acquired (14, 43). However, such individuals are much more frequently infected with vaccinal *M. bovis* BCG or with *M. avium* (16).

We were surprised by the major defect in *M. abscessus* control affecting *Tnf*$^{-/-}$ mice; these mice showed clear bacterial regrowth between days 15 and 21 in the liver, and all animals died within 30 days after the challenge. These results are highly relevant because TNF-deficient mice infected with *M. chelonae* were asymptomatic and the bacterial counts were not significantly different from those in wild-type controls. Similar bacterial counts were obtained in TNF-deficient mice infected intravenously with *M. chelonae* (this study) and *M. smegmatis* (46). This is consistent with the absence of a significant TNF response in *M. chelonae*-infected mice. The only previous descriptions of severe experimental mycobacterial pathogenesis caused by disruption of the TNF pathway involved infections with SGM. Mice selectively deficient in TNFRp55 and intravenously challenged with 5×10^5 CFU of *M. tuberculosis* died within 3 weeks after the challenge (24); similar results were subsequently reported for TNF-deficient mice (31). The profile of *M. avium* infection is closer to that of the *M. abscessus* model, with survival of IFN-γ-deficient animals, death of mice deficient in TNF signaling (TNFRp55 deficient) within a similar time, and bacterial loads otherwise compatible with survival (19). This is consistent with clinical observations; *M. avium* and *M. abscessus* have been reported to cause infections in patients receiving TNF inhibitor therapies (40, 52). TNF plays an important role in the control of mycobacterial growth in tissues by contributing to the early organization and maintenance of the granuloma (46). However, the control of mycobacterial growth in itself cannot explain the lethality observed with *M. abscessus* and *M. avium*, because the bacterial loads at the time of death in TNF- and TNFRp55-deficient mice are lower than the bacterial loads compatible with life in other selectively deficient or wild-type mice (18). It has been reported by Ehlers et al. that death of TNFRp55-deficient mice infected with *M. avium* was caused not by an increased mycobacterial load but by acute granuloma disintegration and destruction of the surrounding tissues (19), a finding consistent with our results. Major thromboembolic lesions may also contribute to the death of animals, as suggested by our premortem pathological observations. However, the histological results of TNF-deficient mouse studies should be interpreted with care, given the potential alterations in tissue architecture in these mice.

Overall, we show here that the immune control of *M. abscessus* exhibits characteristics previously observed in experimental infections with SGM, particularly *M. avium*. Our study confirms the unusual position of *M. abscessus* among the RGM (44) and raises questions about the molecular mechanisms involved in the virulence of this species. We are currently sequencing the entire genome of *M. abscessus* CIP 104536^T,

which should allow decisive progress. Another interesting issue is the dynamics underlying the S-morphotype/R-morphotype variation during infection of a live host by *M. abscessus*. Work is also in progress to address this question.

REFERENCES

1. **Anonymous.** 2004. Tuberculosis associated with blocking agents against tumor necrosis factor-alpha—California, 2002-2003. Morb. Mortal. Wkly. Rep. **53:**683–686.
2. **Billman-Jacobe, H.** 2004. Glycopeptidolipid synthesis in mycobacteria. Curr. Sci. **86:**11–114.
3. **Bolan, G., A. L. Reingold, L. A. Carson, V. A. Silcox, C. L. Woodley, P. S. Hayes, A. W. Hightower, L. McFarland, J. W. Brown III, N. J. Petersen, et al.** 1985. Infections with *Mycobacterium chelonei* in patients receiving dialysis and using processed hemodialyzers. J. Infect. Dis. **152:**1013–1019.
4. **Bosio, C. M., D. Gardner, and K. L. Elkins.** 2000. Infection of B cell-deficient mice with CDC 1551, a clinical isolate of *Mycobacterium tuberculosis*: delay in dissemination and development of lung pathology. J. Immunol. **164:**6417–6425.
5. **Boulman, N., M. Rozenbaum, G. Slobodin, and I. Rosner.** 2006. *Mycobacterium fortuitum* infection complicating infliximab therapy in rheumatoid arthritis. Clin. Exp. Rheumatol. **24:**723.
6. **Brown-Elliott, B. A., and R. J. Wallace, Jr.** 2002. Clinical and taxonomic status of pathogenic nonpigmented or late-pigmenting rapidly growing mycobacteria. Clin. Microbiol. Rev. **15:**716–746.
7. **Byrd, T. F., and C. R. Lyons.** 1999. Preliminary characterization of a *Mycobacterium abscessus* mutant in human and murine models of infection. Infect. Immun. **67:**4700–4707.
8. **Casadevall, A., and L. A. Pirofski.** 2004. New concepts in antibody-mediated immunity. Infect. Immun. **72:**6191–6196.
9. **Casanova, J. L., and L. Abel.** 2002. Genetic dissection of immunity to mycobacteria: the human model. Annu. Rev. Immunol. **20:**581–620.
10. **Catherinot, E., J. Clarissou, G. Etienne, F. Ripoll, J. F. Emile, M. Daffe, C. Perronne, C. Soudais, J. L. Gaillard, and M. Rottman.** 2007. Hypervirulence of a rough variant of the *Mycobacterium abscessus* type strain. Infect. Immun. **75:**1055–1058.
11. **Chetchotisakd, P., P. Mootsikapun, S. Anunnatsiri, K. Jirarattanapochai, C. Choonhakarn, A. Chaiprasert, P. N. Ubol, L. J. Wheat, and T. E. Davis.** 2000. Disseminated infection due to rapidly growing mycobacteria in immunocompetent hosts presenting with chronic lymphadenopathy: a previously unrecognized clinical entity. Clin. Infect. Dis. **30:**29–34.
12. **Colucci, F., C. Soudais, E. Rosmaraki, L. Vanes, V. L. Tybulewicz, and J. P. Di Santo.** 1999. Dissecting NK cell development using a novel alymphoid mouse model: investigating the role of the c-abl proto-oncogene in murine NK cell differentiation. J. Immunol. **162:**2761–2765.
13. **Cooper, A. M., D. K. Dalton, T. A. Stewart, J. P. Griffin, D. G. Russell, and I. M. Orme.** 1993. Disseminated tuberculosis in interferon gamma gene-disrupted mice. J. Exp. Med. **178:**2243–2247.
14. **Doffinger, R., E. Jouanguy, S. Dupuis, M. C. Fondaneche, J. L. Stephan, J. F. Emile, S. Lamhamedi-Cherradi, F. Altare, A. Pallier, G. Barcenas-Morales, E. Meinl, C. Krause, S. Pestka, R. D. Schreiber, F. Novelli, and J. L. Casanova.** 2000. Partial interferon-gamma receptor signaling chain deficiency in a patient with bacille Calmette-Guerin and *Mycobacterium abscessus* infection. J. Infect. Dis. **181:**379–384.
15. **Doherty, T. M., and A. Sher.** 1997. Defects in cell-mediated immunity affect chronic, but not innate, resistance of mice to *Mycobacterium avium* infection. J. Immunol. **158:**4822–4831.
16. **Dorman, S. E., C. Picard, D. Lammas, K. Heyne, J. T. van Dissel, R. Baretto, S. D. Rosenzweig, M. Newport, M. Levin, J. Roesler, D. Kumararatne, J. L. Casanova, and S. M. Holland.** 2004. Clinical features of dominant and recessive interferon gamma receptor 1 deficiencies. Lancet **364:**2113–2121.
17. **Dunn, P. L., and R. J. North.** 1995. Virulence ranking of some *Mycobacterium tuberculosis* and *Mycobacterium bovis* strains according to their ability to multiply in the lungs, induce lung pathology, and cause mortality in mice. Infect. Immun. **63:**3428–3437.
18. **Ehlers, S., J. Benini, S. Kutsch, R. Endres, E. T. Rietschel, and K. Pfeffer.** 1999. Fatal granuloma necrosis without exacerbated mycobacterial growth in tumor necrosis factor receptor p55 gene-deficient mice intravenously infected with *Mycobacterium avium*. Infect. Immun. **67:**3571–3579.

19. **Ehlers, S., S. Kutsch, E. M. Ehlers, J. Benini, and K. Pfeffer.** 2000. Lethal granuloma disintegration in mycobacteria-infected TNFRp55$^{-/-}$ mice is dependent on T cells and IL-12. J. Immunol. **165:**483–492.

20. **Ehlers, S., and E. Richter.** 2001. Differential requirement for interferongamma to restrict the growth of or eliminate some recently identified species of nontuberculous mycobacteria in vivo. Clin. Exp. Immunol. **124:**229–238.

21. **Falkinham, J. O., III.** 1996. Epidemiology of infection by nontuberculous mycobacteria. Clin. Microbiol. Rev. **9:**177–215.

22. **Flynn, J. L., and J. Chan.** 2001. Immunology of tuberculosis. Annu. Rev. Immunol. **19:**93–129.

23. **Flynn, J. L., J. Chan, K. J. Triebold, D. K. Dalton, T. A. Stewart, and B. R. Bloom.** 1993. An essential role for interferon gamma in resistance to *Mycobacterium tuberculosis* infection. J. Exp. Med. **178:**2249–2254.

24. **Flynn, J. L., M. M. Goldstein, J. Chan, K. J. Triebold, K. Pfeffer, C. J. Lowenstein, R. Schreiber, T. W. Mak, and B. R. Bloom.** 1995. Tumor necrosis factor-alpha is required in the protective immune response against *Mycobacterium tuberculosis* in mice. Immunity **2:**561–572.

25. **Fraser, V. J., M. Jones, P. R. Murray, G. Medoff, Y. Zhang, and R. J. Wallace, Jr.** 1992. Contamination of flexible fiberoptic bronchoscopes with *Mycobacterium chelonae* linked to an automated bronchoscope disinfection machine. Am. Rev. Respir. Dis. **145:**853–855.

26. **Griffith, D. E., W. M. Girard, and R. J. Wallace, Jr.** 1993. Clinical features of pulmonary disease caused by rapidly growing mycobacteria. An analysis of 154 patients. Am. Rev. Respir. Dis. **147:**1271–1278.

27. **Huang, S., W. Hendriks, A. Althage, S. Hemmi, H. Bluethmann, R. Kamijo, J. Vilcek, R. M. Zinkernagel, and M. Aguet.** 1993. Immune response in mice that lack the interferon-gamma receptor. Science **259:**1742–1745.

28. **Ingram, C. W., D. C. Tanner, D. T. Durack, G. W. Kernodle, Jr., and G. R. Corey.** 1993. Disseminated infection with rapidly growing mycobacteria. Clin. Infect. Dis. **16:**463–471.

29. **Johnson, C. M., A. M. Cooper, A. A. Frank, C. B. Bonorino, L. J. Wysoki, and I. M. Orme.** 1997. *Mycobacterium tuberculosis* aerogenic rechallenge infections in B cell-deficient mice. Tuber. Lung Dis. **78:**257–261.

30. **Kamijo, R., J. Le, D. Shapiro, E. A. Havell, S. Huang, M. Aguet, M. Bosland, and J. Vilcek.** 1993. Mice that lack the interferon-gamma receptor have profoundly altered responses to infection with Bacillus Calmette-Guerin and subsequent challenge with lipopolysaccharide. J. Exp. Med. **178:**1435–1440.

31. **Kaneko, H., H. Yamada, S. Mizuno, T. Udagawa, Y. Kazumi, K. Sekikawa, and I. Sugawara.** 1999. Role of tumor necrosis factor-alpha in *Mycobacterium*-induced granuloma formation in tumor necrosis factor-alpha-deficient mice. Lab. Investig. **79:**379–386.

32. **Khader, S. A., J. E. Pearl, K. Sakamoto, L. Gilmartin, G. K. Bell, D. M. Jelley-Gibbs, N. Ghilardi, F. deSauvage, and A. M. Cooper.** 2005. IL-23 compensates for the absence of IL-12p70 and is essential for the IL-17 response during tuberculosis but is dispensable for protection and antigenspecific IFN-gamma responses if IL-12p70 is available. J. Immunol. **175:**788–795.

33. **Kitada, S., R. Maekura, N. Toyoshima, N. Fujiwara, I. Yano, T. Ogura, M. Ito, and K. Kobayashi.** 2002. Serodiagnosis of pulmonary disease due to *Mycobacterium avium* complex with an enzyme immunoassay that uses a mixture of glycopeptidolipid antigens. Clin. Infect. Dis. **35:**1328–1335.

34. **Kitamura, D., J. Roes, R. Kuhn, and K. Rajewsky.** 1991. A B cell-deficient mouse by targeted disruption of the membrane exon of the immunoglobulin mu chain gene. Nature **350:**423–426.

35. **Kubica, G. P., I. Baess, R. E. Gordon, P. A. Jenkins, J. B. Kwapinski, C. McDurmont, S. R. Pattyn, H. Saito, V. Silcox, J. L. Stanford, K. Takeya, and M. Tsukamura.** 1972. A co-operative numerical analysis of rapidly growing mycobacteria. J. Gen. Microbiol. **73:**55–70.

36. **Kusunoki, S., and T. Ezaki.** 1992. Proposal of *Mycobacterium peregrinum* sp. nov., nom. rev., and elevation of *Mycobacterium chelonae* subsp. *abscessus* (Kubica et al.) to species status: *Mycobacterium abscessus* comb. nov. Int. J. Syst. Bacteriol. **42:**240–245.

37. **Malissen, M., A. Gillet, L. Ardouin, G. Bouvier, J. Trucy, P. Ferrier, E. Vivier, and B. Malissen.** 1995. Altered T cell development in mice with a targeted mutation of the CD3-epsilon gene. EMBO J. **14:**4641–4653.

38. **Marie, I., P. Heliot, F. Roussel, F. Herve, J. F. Muir, and H. Levesque.** 2005. Fatal *Mycobacterium peregrinum* pneumonia in refractory polymyositis treated with infliximab. Rheumatology (Oxford) **44:**1201–1202.

39. **Marino, M. W., A. Dunn, D. Grail, M. Inglese, Y. Noguchi, E. Richards, A. Jungbluth, H. Wada, M. Moore, B. Williamson, S. Basu, and L. J. Old.** 1997. Characterization of tumor necrosis factor-deficient mice. Proc. Natl. Acad. Sci. USA **94:**8093–8098.

40. **Mufti, A. H., B. W. Toye, R. R. McKendry, and J. B. Angel.** 2005. *Mycobacterium abscessus* infection after use of tumor necrosis factor alpha inhibitor therapy: case report and review of infectious complications associated with tumor necrosis factor alpha inhibitor use. Diagn. Microbiol. Infect. Dis. **53:**233–238.

41. **North, R. J., and A. A. Izzo.** 1993. Mycobacterial virulence. Virulent strains of *Mycobacteria tuberculosis* have faster in vivo doubling times and are better equipped to resist growth-inhibiting functions of macrophages in the presence and absence of specific immunity. J. Exp. Med. **177:**1723–1733.

42. **Overbergh, L., D. Valckx, M. Waer, and C. Mathieu.** 1999. Quantification of murine cytokine mRNAs using real time quantitative reverse transcriptase PCR. Cytokine **11:**305–312.

43. **Patel, S. Y., L. Ding, M. R. Brown, L. Lantz, T. Gay, S. Cohen, L. A. Martyak, B. Kubak, and S. M. Holland.** 2005. Anti-IFN-gamma autoantibodies in disseminated nontuberculous mycobacterial infections. J. Immunol. **175:**4769–4776.

44. **Petrini, B.** 2006. *Mycobacterium abscessus*: an emerging rapid-growing potential pathogen. APMIS **114:**319–328.

45. **Ringuet, H., C. Akoua-Koffi, S. Honore, A. Varnerot, V. Vincent, P. Berche, J. L. Gaillard, and C. Pierre-Audigier.** 1999. *hsp65* sequencing for identification of rapidly growing mycobacteria. J. Clin. Microbiol. **37:**852–857.

46. **Roach, D. R., A. G. Bean, C. Demangel, M. P. France, H. Briscoe, and W. J. Britton.** 2002. TNF regulates chemokine induction essential for cell recruitment, granuloma formation, and clearance of mycobacterial infection. J. Immunol. **168:**4620–4627.

47. **Saito, H., and H. Tasaka.** 1969. Comparison of the pathogenicity for mice of *Mycobacterium fortuitum* and *Mycobacterium abscessus*. J. Bacteriol. **99:**851–855.

48. **Sanguinetti, M., F. Ardito, E. Fiscarelli, M. La Sorda, P. D'Argenio, G. Ricciotti, and G. Fadda.** 2001. Fatal pulmonary infection due to multidrugresistant *Mycobacterium abscessus* in a patient with cystic fibrosis. J. Clin. Microbiol. **39:**816–819.

49. **Scollard, D. M., M. P. Joyce, and T. P. Gillis.** 2006. Development of leprosy and type 1 leprosy reactions after treatment with infliximab: a report of 2 cases. Clin. Infect. Dis. **43:**e19–e22.

50. **Sermet-Gaudelus, I.** 2003. *Mycobacterium abscessus* and children with cystic fibrosis. Emerg. Infect. Dis. **9:**1587–1591.

51. **Shinkai, Y., G. Rathbun, K. P. Lam, E. M. Oltz, V. Stewart, M. Mendelsohn, J. Charron, M. Datta, F. Young, A. M. Stall, et al.** 1992. RAG-2-deficient mice lack mature lymphocytes owing to inability to initiate V(D)J rearrangement. Cell **68:**855–867.

52. **Thomas, J. E., C. R. Taoka, B. T. Gibbs, and S. L. Fraser.** 2006. Fatal pulmonary *Mycobacterium abscessus* infection in a patient using etanercept. Hawaii Med. J. **65:**12–15.

53. **Tomashefski, J. F., Jr., R. C. Stern, C. A. Demko, and C. F. Doershuk.** 1996. Nontuberculous mycobacteria in cystic fibrosis. An autopsy study. Am. J. Respir. Crit. Care Med. **154:**523–528.

54. **Villanueva, A., R. V. Calderon, B. A. Vargas, F. Ruiz, S. Aguero, Y. Zhang, B. A. Brown, and R. J. Wallace, Jr.** 1997. Report on an outbreak of postinjection abscesses due to *Mycobacterium abscessus*, including management with surgery and clarithromycin therapy and comparison of strains by random amplified polymorphic DNA polymerase chain reaction. Clin. Infect. Dis. **24:**1147–1153.

55. **Vordermeier, H. M., N. Venkataprasad, D. P. Harris, and J. Ivanyi.** 1996. Increase of tuberculous infection in the organs of B cell-deficient mice. Clin. Exp. Immunol. **106:**312–316.

56. **Wallace, R. J., Jr., B. A. Brown, and D. E. Griffith.** 1997. *Mycobacterium chelonae vs. abscessus.* Pediatr. Infect. Dis. J. **16:**829.

57. **Wallace, R. J., Jr., Y. Zhang, B. A. Brown, V. Fraser, G. H. Mazurek, and S. Maloney.** 1993. DNA large restriction fragment patterns of sporadic and epidemic nosocomial strains of *Mycobacterium chelonae* and *Mycobacterium abscessus*. J. Clin. Microbiol. **31:**2697–2701.

Editor: J. L. Flynn